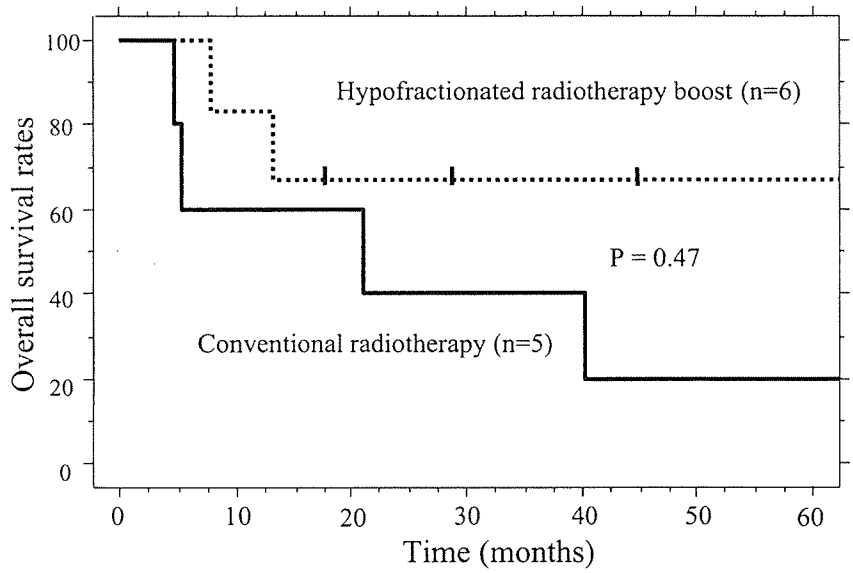

Figure 3. The actuarial survival curves for patients who received conventional radiotherapy and for patients who received hypofractionated radiotherapy boost for dose escalation.

The patient tolerated the surgery for the relapsed tumor without serious complications.

Discussion

In many cases, spinal ependymoma can be totally resected, and often no irradiation is required after the surgery [4,17,18]. However, for patients who receive a partial resection, or have a tumor with a high proliferation index [17], post-operative radiotherapy has been recommended to reduce relapse of the tumor [4]. Gilhuis et al. [6] reported that three out of three patients who did not receive radiotherapy relapsed, whereas three out of eleven patients who received radiotherapy relapsed after a partial resection of the ependymoma. Total resection is usually impossible for myxopapillary ependymoma, which often has residual disease or dissemination at the cauda equina. Gilhuis et al. [6] showed that three out of three patients who did not receive radiotherapy relapsed, whereas one out of nine who received radiotherapy relapsed. We have not seen any relapse of the tumor when we used a radiation field that covered the cauda equina. Since we have seen a relapse at the cauda equina in one girl who did not receive irradiation for the cauda equina, and had only been treated on the tumor bed after a partial resection of a myxopapillary ependymoma, we strongly recommend that the cauda equina be included as the clinical target volume for this disease. The results in this study showed that conventional radiotherapy after the partial resection of ependymal tumors did not increase morbidity. The survival rate at 5 years was 93% in 18 patients in Linstadt et al.'s series [12], 83% in 59 patients in Waldron et al.'s series [3], 100% in 10 patients in McLaughlin et al.'s series [2], 97% in 35 patients in Schild et al.'s series [19], and 94% in 25 patients in Wahab et al.'s series [5] (Table 4A). The actuarial survival rates at 5 and 10 years were 94% and 84%, respectively, for the ependymal tumors in our series, which is consistent with the other reports.

The actuarial overall survival rates of 5 and 10 years for astrocytic tumors were 54% and 47%, respectively. This is consistent with the previous reports: the 5-year survival rates were 53% in 15 patients in Linstadt et al.'s series [12], 55% in 23 patients in Jyothirmayi et al.'s series [10], 58% in 12 patients in McLaughlin et al.'s series [2], 64% in 24 patients in Wahab et al.'s series [5], and 54% in 52 patients in Rodrigues et al.'s series [1] (Table 4B). The 5- and 10-year actuarial survival rates were 68% and 57% for low-grade astrocytic tumors, which was lower than for ependymal tumors. Long-term morbidity due to adjuvant conventional radiotherapy was shown to be minimal. Post-operative radiotherapy for a low-grade astrocytoma is a reasonable option, with a possibly

Table 4. Result of post-operative radiation therapy for spinal cord (A) ependymal tumors; (B) astrocytic tumors; (C) high-grade astrocytic tumors

Author (year)	Patients	5-year survival rates (%)
(A)		
Linstadt et al. (1989)	18	93
Waldron et al. (1993)	59	83
McLaughlin et al. (1998)	10	100
Schild et al. (1998)	35	97
Wahab et al. (1999)	25	94
(B)		
Linstadt et al. (1989)	15	53
Jyothirmayi et al. (1997)	23	55
McLaughlin et al. (1998)	12	58
Wahab et al. (1999)	24	64
Rodrigues et al. (2000)	52	54
(C)		
Linstadt et al. (1989)	3	0
Cohen et al. (1989)	19	0
Jyothirmayi et al. (1997)	6	0
McLaughlin et al. (1998)	4	24
Rodrigues et al. (2000)	15	20

increased progression-free rate [20]. It may not be necessary to use ionizing irradiation on pediatric patients if a total gross resection has been achieved [8]. The scale for the assessment of neurological outcome in this study can be criticized to be to too simple and we hope to analyze the sensorimotor function using more precise scale in a prospective study in near future.

The results of the high-grade gliomas in the literature are all dismal (Table 4C). Of the 6 patients in Jyothirmayi et al.'s series [10], none survived more than 2 years. Of the 3 patients in Linstadt et al.'s series [12], none survived more than 8 months. The median survival was 6 months following surgery in 19 patients in Cohen et al.'s series [9]. The 5-year progression-free survival was 20% in the 15 patients in Rodrigues et al.'s series [1]. In our series, the projected actuarial 5-year survival rates of high-grade glioma were 35%, and, particularly for patients treated with hypofractionated radiotherapy boost for dose escalation, the projected actuarial 5-year survival rates were 67%. Because of careful treatment planning, no serious non-spinal cord injuries such as renal failure or skin ulcers were observed. The severe subcutaneous skin induration and pruritus in the initial patient after posterior single field irradiation could have been avoided if a more sophisticated treatment had been used. Sensorimotor dysfunction was acceptable for the rest of the patients. For the patient with good motor function before treatment, the decision to get a hypofractionated radiotherapy boost had been a difficult one. However, that patient was fully employed at 45 months after surgery, and had accepted the decision as the right one. The appropriate margin for this treatment may be larger than the T2-high region considering the marginal relapse in our series. Kyoshima et al. [21] have reported about the surgical cordotomy for a patient with spinal high-grade astrocytic tumor. They showed that the tumor infiltrated more rostrally within the parenchyma of the spinal cord than the level indicated by a T2-weighted MR image [21], which is consistent with our pathological findings at the relapse.

Although the number of patients was too small to come to definitive conclusions, the preliminary outcome of the hypofractionated radiotherapy boost for dose escalation was encouraging. Further investigation is required to confirm the benefit and indication of this treatment. Surgical cordotomy may also provide the similar results in survival but the latency between the treatment and the loss of the neurological function in our method would be preferable for the quality of life. Patients with dissemination or a tumor in the cervical spine would not be candidates for this treatment. Recent advances in radiotherapy, such as intensity-modulated radiotherapy or particle therapy with careful monitoring of the patient position, would make it easier to concentrate the dose to the spinal cord, without causing damage to the surrounding normal tissues [22,23]. The most important step to take when considering this treatment is a pathological diagnosis by neuro-pathologists, and sufficient agreement concerning ethical considerations from the community as well as from the patient.

References

1. Rodrigues GB, Waldron JN, Wong CS, Laperriere NJ: A retrospective analysis of 52 cases of spinal cord glioma managed with radiation therapy. Int J Radiat Oncol Biol Phys 48: 837–842, 2000
2. McLaughlin MP, Buatti JM, Marcus RB Jr., Maria BL, Mickle PJ, Kedar A: Outcome after radiotherapy of primary spinal cord glial tumors. Radiat Oncol Investig 6: 276–280, 1998
3. Waldron JN, Laperriere NJ, Jaakkimainen L, Simpson WJ, Payne D, Milosevic M, Wong CS: Spinal cord ependymomas: a retrospective analysis of 59 cases. Int J Radiat Oncol Biol Phys 27: 223–229, 1993
4. Shirato H, Kamada T, Hida K, Koyanagi I, Iwasaki Y, Miyasaka K, Abe H: The role of radiotherapy in the management of spinal cord glioma. Int J Radiat Oncol Biol Phys 33: 323–328, 1995
5. Abdel-Wahab M, Corn B, Wolfson A, Raub W, Gaspar LE, Curran W Jr, Bustillo P, Rubinton P, Markoe A: Prognostic factors and survival in patients with spinal cord gliomas after radiation therapy. Am J Clin Oncol 22: 344–351, 1999
6. Gilhuis HJ, Kappelle AC, Beute G, Wesseling P, Grotenhuis A, Boerman RH: Radiotherapy for partially resected spinal ependymomas: a retrospective study of 60 cases. Oncol Rep 10: 2079–2082, 2003
7. Minehan KJ, Shaw EG, Scheithauer BW, Davis DL, Onofrio BM: Spinal cord astrocytoma: pathological and treatment considerations. J Neurosurg 83: 590–595, 1995
8. Przybylski GJ, Albright AL, Martinez AJ: Spinal cord astrocytomas: long-term results comparing treatments in children. Childs Nerv Syst 13: 375–382, 1997
9. Cohen AR, Wisoff JH, Allen JC, Epstein F: Malignant astrocytomas of the spinal cord. J Neurosurg 70: 50–54, 1989
10. Jyothirmayi R, Madhavan J, Nair MK, Rajan B: Conservative surgery and radiotherapy in the treatment of spinal cord astrocytoma. J Neurooncol 33: 205–211, 1997
11. Kopelson G, Linggood RM, Kleinman GM, Doucette J, Wang CC: Management of intramedullary spinal cord tumors. Radiology 135: 473–479, 1980
12. Linstadt DE, Wara WM, Leibel SA, Gutin PH, Wilson CB, Sheline GE: Postoperative radiotherapy of primary spinal cord tumors. Int J Radiat Oncol Biol Phys 16: 1397–1403, 1989
13. Allen JC, Aviner S, Yates AJ, Boyett JM, Cherlow JM, Turski PA, Epstein F, Finlay JL: Treatment of high-grade spinal cord astrocytoma of childhood with "8-in-1" chemotherapy and radiotherapy: a pilot study of CCG-945. Children's Cancer Group. J Neurosurg 88: 215–220, 1998
14. Loeffler JS, Alexander E 3rd, Shea WM, Wen PY, Fine HA, Kooy HM, Black PM: Radiosurgery as part of the initial management of patients with malignant gliomas. J Clin Oncol 10: 1379–1385, 1992
15. Hall WA, Djalilian HR, Sperduto PW, Cho KH, Gerbi BJ, Gibbons JP, Rohr M, Clark HB: Stereotactic radiosurgery for recurrent malignant gliomas. J Clin Oncol 13: 1642–1648, 1995
16. Regine WF, Patchell RA, Strottmann JM, Meigooni A, Sanders M, Young AB: Preliminary report of a phase I study of combined fractionated stereotactic radiosurgery and conventional external beam radiation therapy for unfavorable gliomas. Int J Radiat Oncol Biol Phys 48: 421–426, 2000
17. Iwasaki Y, Hida K, Sawamura Y, Abe H.: Spinal intramedullary ependymomas: surgical results and immunohistochemical analysis of tumour proliferation activity. Br J Neurosurg 14: 331–336, 2000
18. Hoshimaru M, Koyama T, Hashimoto N, Kikuchi H: Results of microsurgical treatment for intramedullary spinal cord ependymomas: analysis of 36 cases. Neurosurgery 44: 264–269, 1999
19. Schild SE, Nisi K, Scheithauer BW, Wong WW, Lyons MK, Schomberg PJ, Shaw EG: The results of radiotherapy for ependymomas: the Mayo Clinic experience. Int J Radiat Oncol Biol Phys 42: 953–958, 1998
20. Kim MS, Chung CK, Choe G, Kim IH, Kim HJ: Intramedullary spinal cord astrocytoma in adults: postoperative outcome. J Neurooncol 52: 85–94, 2001

21. Kyoshima K, Ito K, Tanabe A, Iwashita T, Goto T, Sato A, Nakayama J: Malignant astrocytoma of the conus medullaris treated by spinal cordectomy. J Clin Neurosci 9: 211–216, 2002
22. Miralbell R, Lomax A, Russo M.: Potential role of proton therapy in the treatment of pediatric medulloblastoma/primitive neuroectodermal tumors: spinal theca irradiation. Int J Radiat Oncol Biol Phys 38: 805–811, 1997
23. Milker-Zabel S, Zabel A, Thilmann C, Schlegel W, Wannenmacher M, Debus J: Clinical results of retreatment of vertebral bone metastases by stereotactic conformal radiotherapy and intensity-modulated radiotherapy. Int J Radiat Oncol Biol Phys 55: 162-167, 2003

Address for offprints: Norio Katoh, Department of Radiology, Hokkaido University School of Medicine, North-15 West-7, Kita-ku, 060-8638, Sapporo, Japan; Tel.: +81-11-716-1161; Fax: +81-11-706-7876; E-mail: noriwo@radi.med.hokudai.ac.jp

J Neurooncol
DOI 10.1007/s11060-006-9247-5

LABORATORY INVESTIGATION

Safety and efficacy of convection-enhanced delivery of ACNU, a hydrophilic nitrosourea, in intracranial brain tumor models

Shin-ichiro Sugiyama · Yoji Yamashita · Toshio Kikuchi · Ryuta Saito · Toshihiro Kumabe · Teiji Tominaga

Received: 21 June 2006 / Accepted: 11 August 2006

Abstract Convection-enhanced delivery (CED) is a local infusion technique, which delivers chemotherapeutic agents directly to the central nervous system, circumventing the blood–brain barrier and reducing systemic side effects. CED distribution is significantly increased if the infusate is hydrophilic. This study evaluated the safety and efficacy of CED of nimustine hydrochloride: 3-[(4-amino-2-methyl-5-pyrimidinyl) methyl]-1-(2-chloroethyl)-1-nitrosourea hydrochloride (ACNU), a hydrophilic nitrosourea, in rat 9 L brain tumor models. The local neurotoxicity of ACNU delivered via CED was examined in normal rat brains, and the maximum tolerated dose (MTD) was estimated at 0.02 mg/rat. CED of ACNU at the MTD produced significantly longer survival time than systemic administration ($P < 0.05$, log-rank test). Long-term survival (80 days) and eradication of the tumor occurred only in the CED-treated rats. The tissue concentration of ACNU was measured by high-performance liquid chromatography, which revealed that CED of ACNU at the dose of 100-fold less total drug than intravenous injection carried almost equivalent concentrations of ACNU into rat brain tissue. CED of hydrophilic ACNU is a promising strategy for treating brain tumors.

Keywords Brain tumor · Convection-enhanced delivery · High-performance liquid chromatography · Nimustine hydrochloride · Nitrosourea

S. Sugiyama · Y. Yamashita (✉) ·
T. Kikuchi · R. Saito · T. Kumabe · T. Tominaga
Department of Neurosurgery, Tohoku University Graduate School of Medicine, 1-1 Seiryo-machi, Aoba-ku, Sendai 980-8574, Japan
e-mail: yoji@nsg.med.tohoku.ac.jp

Abbreviations

ACNU	3-[(4-amino-2-methyl-5-pyrimidinyl) methyl]-1-(2-chloroethyl)-1-nitrosourea hydrochloride
BBB	Blood-brain barrier
BCNU	1,3-bis-chlorethyl-1-nitrosourea
CED	Convection-enhanced delivery
CNS	Central nervous system
HBSS	Hanks balanced salt solution
H&E	Hematoxylin and eosin
i.v.	Intravenous
MTD	Maximum tolerated dose

Introduction

Prognosis for the patients with high-grade gliomas remains dismal. Recently, Stupp et al. [1] demonstrated that radiotherapy plus concomitant and adjuvant temozolomide, a novel oral alkylating agent, is well tolerated and improves survival in patients with newly diagnosed glioblastoma. However, the activity of temozolomide is still not satisfactory in malignant gliomas. Poor penetration of most anti-cancer drugs across the blood–brain barrier (BBB) into the central nervous system (CNS) remains a major obstacle in the application of systemic chemotherapy for intracranial malignancies [2, 3]. Even using agents that penetrate the BBB, tumoricidal drug concentrations are difficult to reach brain tumor tissue without incurring unacceptable systemic side effects.

Convection-enhanced delivery (CED) was introduced in 1994 as a strategy to overcome such difficulties

[4]. Utilizing bulk flow, CED allows the direct delivery of small or large molecules to a targeted site, offering an improved volume of distribution compared to simple diffusion. CED bypasses the BBB, delivers a high concentration of therapeutic agents to the injection site, provides wider distribution of therapeutic agents within the target site, and minimizes systemic exposure, resulting in fewer systemic side effects. In addition, CED provides homogeneous distribution of infusate, which drop off sharply at the edge in normal brain tissue, resulting in delivery of the therapeutic agent to the entire targeted region while limiting the potential for widespread neurotoxicity [5].

Nitrosoureas have been important in systemic chemotherapy for high-grade gliomas for decades. 1,3-bischlorethyl-1-nitrosourea (BCNU) had the most proven efficacy, but the effects on clinical outcome have been limited [6]. Dose escalation of BCNU to increase the efficacy against gliomas has been hampered by severe systemic toxicity to the bone marrow, lungs, and kidneys [7]. To avoid such systemic toxicities, local delivery methods, including direct injection and biodegradable polymers or wafers, have been used, but only offered modest improvements to the overall survival rates for patients with malignant gliomas [8–13]. Those delivery methods yielded limited diffusion and distribution of drug into the surrounding tissues, which is typically not more than a few millimeters [13].

Convection-enhanced delivery has the potential to deliver an efficient volume of BCNU to targeted sites without systemic exposure. BCNU could be safely and effectively administered via CED in the rat glioma model to shrink gliomas with little or no toxicity [14]. However, BCNU is not the ideal drug for CED because the log p of BCNU is 1.53, which means that BCNU is lipophilic [15] (log p is the log of the octanol/water partition coefficient [16]). For CED injection, it needs to dissolve in organic solvent like ethanol that has nonspecific cytotoxity in itself. Furthermore, the water solubility of drugs limits the volume of distribution within the brain tissue and CED distributed lipophilic drugs less widely than hydrophilic agents [11, 12].

3-[(4-amino-2-methyl-5-pyrimidinyl) methyl]-1-(2-chloroethyl)-1-nitorosourea hydrochloride (ACNU), is the first water-soluble nitrosourea compound discovered in 1974 [17]. ACNU dissolves in water easily as a cationic ion. The log p of ACNU is 0.92 [17], which means that ACNU is lipophilic as well as hydrophilic, because ACNU changes from cationic ion to neutral compound under physiological conditions. In clinical protocols against high-grade gliomas, systemic administration of ACNU has proven efficacy but also dose-limiting myelotoxicity like BCNU [18, 19].

We hypothesized that CED of ACNU would be therapeutically advantageous over systemic administration for treating intracranial malignancies, because CED could distribute hydrophilic ACNU over the entire targeted region and deliver a high concentration of ACNU without systemic exposure. This study examined the safety and efficacy of CED with ACNU in rat 9 L brain tumor models.

Materials and methods

ACNU

ACNU was provided by Sankyo Co. Ltd. (Tokyo, Japan). Infusion solutions of ACNU were prepared by diluting ACNU in saline to a concentration of 10, 5, 2, 1, 0.5, 0.2, and 0.1 mg/mL.

Tumor cell line

The 9 L gliosarcoma cells (American Type Culture Collection, Rockville, MD, USA) were maintained as monolayers in a complete medium consisting of Eagle's minimal essential medium supplemented with 10% fetal calf serum, non-essential amino acids, and 100 U/mL penicillin G. Cells were cultured at 37°C in a humidified atmosphere consisting of 95% air and 5% CO_2.

Animals and intracranial xenograft technique

All protocols used in the animal studies were approved by the Institute for Animal Experimentation of Tohoku University Graduate School of Medicine.

Male Fisher 344 rats weighing approximately 200 g were purchased from Charles-River Laboratories (Charles-River Japan Inc., Tsukuba, Japan). For the intracranial xenograft tumor model, 9 L gliosarcoma cells were harvested by trypsinization, washed once with Hanks balanced salt solution without Ca^{++} and Mg^{++} (HBSS), and resuspended in HBSS for implantation. Cells (5×10^5) in 10 μL HBSS were implanted into the striatal region of Fisher 344 rat brains as follows: under deep isoflurane anesthesia, rats were placed in a small-animal stereotactic frame (David Kopf Instrument, Tujunga, CA, USA). A sagittal incision was made to expose the cranium followed by a burr hole in the skull at 0.5 mm anterior and 3 mm lateral from the bregma using a small dental drill. Cell suspension (5 μL) was injected over 2 min at a depth of 4.5 mm from the brain surface; after a 2-minute wait, another 5 μL were injected over 2 min at a depth of

4.0 mm, and after a final 2-minute wait, the needle was removed and the wound was sutured.

CED

Convection-enhanced delivery of ACNU or saline was done using a volume of 20 μL as described previously [20]. Briefly, the infusion system consisted of a reflux-free step-design infusion cannula (as described [21]) connected to a loading line (containing ACNU or saline) and an olive oil infusion line. A 1-mL syringe (filled with oil) mounted onto a micro-infusion pump (BeeHive; Bioanalytical Systems, West Lafayette, IN, USA) regulated the flow of fluid through the system. Based on chosen coordinates, the infusion cannula was mounted onto stereotactic holders and guided to the target region of the brain through burr holes made in the skull. The following ascending infusion rates were applied to achieve the 20-μL total infusion volume: 0.2 μL/min (15 min) + 0.5 μL/min (10 min) + 0.8 μL/min (15 min).

Evaluation of toxicity

Healthy male Sprague–Dawley rats weighing approximately 200 g (Charles-River Japan Inc.) received a single 20-μL CED infusion of ACNU at doses of 0.2, 0.1, 0.04, 0.02, 0.01, 0.004, or 0.002 mg/rat (six per group). Rats were monitored daily for survival, weekly weights, and general health (alertness, grooming, feeding, excreta, skin, fur, mucous membrane conditions, ambulation, breathing, and posture). Three rats in each group were euthanized on the 30th or the 60th day after the CED treatment, and their brains were removed, fixed, subjected to paraffin sectioning (5 μm), and stained with hematoxylin and eosin (H&E).

Survival studies

Forty rats with 9 L tumor cells were randomly assigned to five groups: (a) the control group, receiving CED of saline ($n = 8$); (b) the systemic treatment group, receiving intravenous (i.v.) injection of ACNU at a dose of 0.4 mg/rat (2 mg/kg: clinically tolerable dose for i.v. administration [17]) ($n = 8$); and (c)–(e) CED groups, receiving CED of ACNU at a dose of 0.005 mg/rat ($n = 8$), 0.01 mg/rat ($n = 8$), and 0.02 mg/rat ($n = 8$). Seven days after tumor cell implantation, a single CED infusion (20 μL; 1 mg/mL or 0.5 mg/mL ACNU) or a bolus i.v. injection via a tail vein (0.4 mL; 0.1 mg/mL ACNU) was performed for each group. Rats were monitored daily for survival and general health. Animal weights were reported weekly. The study was terminated 80 days after tumor implantation, when the surviving animals were euthanized and their brains stained with H&E.

Results for the survival studies are expressed as a Kaplan–Meier curve. Survival between the treatment groups was compared with a log-rank test.

High-performance liquid chromatography for ACNU in rat brain tissue

Normal Sprague–Dawley rats weighing approximately 200 g (Charles-River Japan Inc.) were given a single 20-μL infusion by CED of ACNU at 0.02 mg/rat or a bolus i.v. injection of ACNU at 2.0 mg/rat or 0.4 mg/rat (nine rats per group). Three rats were sacrificed at 0, 2, or 4 h after the treatments. The appropriate brain hemisphere was perfused with phosphate buffered saline, surgically removed, and frozen. All samples were stored at -80°C to avoid deterioration until biochemical measurements were carried out (within a month of brain dissection). Phosphoric acid buffer (0.1 mol/L) was added to the tissues at an 80% ratio (v/w), and the tissue was homogenized using a mechanical homogenizer. Fluoranthene (0.8 μg, internal standard) and *n*-hexane (5 mL) was added to the homogenates (0.5 mL). The mixture was shaken for 5 min and centrifuged at 3,000 rpm for 5 min, then the *n*-hexane layer was extracted and evaporated. The remnant was dissolved in 6% acetonitrile (200 μL) and injected into the chromatographic column (4.6 × 150 mm^2; Nova-Pack C18; Waters, Milford, MA, USA). Analysis was conducted on LC-10A system (Shimadzu Co., Kyoto, Japan). The mobile phase consisted of 6% acetonitrile, refined water, and 1 g/L sodium heptanesulphonate (PIC B7) (77 : 23 : 0.4). All separations were performed isocratically at a flow rate of 1.0 mL/min at room temperature. ACNU was typically eluted in 3 min, and detected by ultraviolet at 254 nm.

Results

Toxicity of ACNU in normal rodent CNS

Dose-limiting local toxicity occurred at 0.04 mg/rat or over, establishing the maximum tolerated dose (MTD) at 0.02 mg/rat (Fig. 1). All animals that received CED of ACNU at 0.04 mg/rat or over had extensive tissue necrosis within the CNS (Fig. 1a). Animals receiving CED of ACNU at 0.02 mg/rat or under showed evidence of minor trauma at the site of the infusion cannula in the striatum but otherwise no apparent tissue toxicity (Fig. 1b, c).

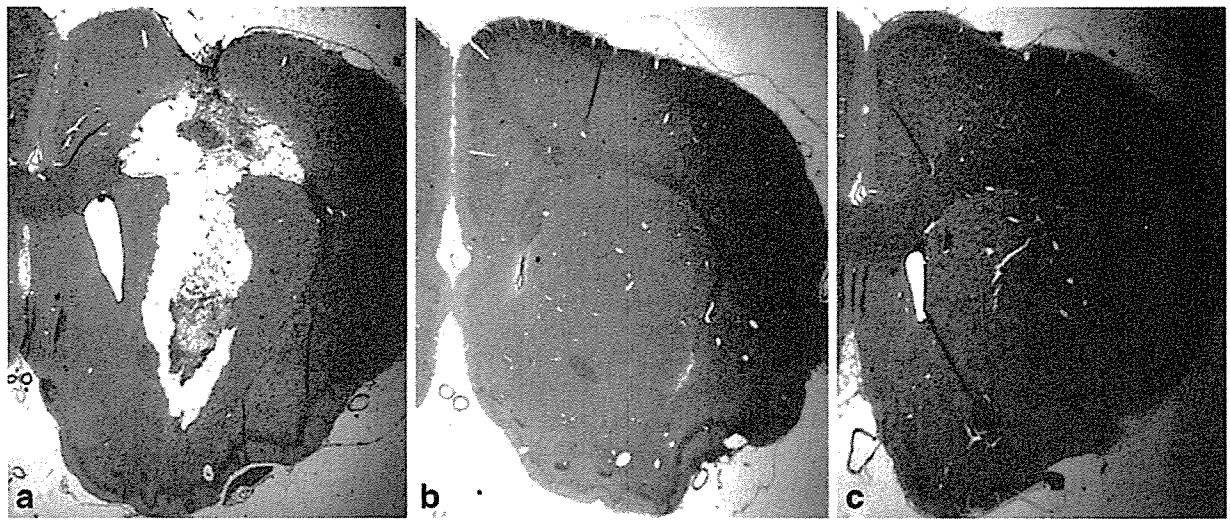

Fig. 1 Local tissue toxicity of ACNU administered via CED in the normal adult rat brain. Rat brains were treated with a single CED infusion of ACNU at different seven doses (0.2, 0.1, 0.04, 0.02, 0.01, 0.004, or 0.002 mg/rat). Representative H&E sections from three groups on the 30th day after CED. Extensive tissue injury was observed in animals treated with more than 0.04 mg/rat (**a**: 0.1 mg/rat). Rats treated with less than 0.02 mg showed no drug-induced damages (**b**: 0.02 mg/rat, **c**: 0.01 mg/rat)

No systemic toxicities were observed following CED of ACNU even at or over MTD. Furthermore, even the extensive CNS damage caused by ACNU resulted in no neurological symptoms.

Anti-tumor efficacy of ACNU through CED or intravenous administration

The anti-tumor efficacy of ACNU delivered via CED at the tested MTD (0.02 mg/rat) and half MTD (0.01 mg/rat) was compared with that of ACNU administered systemically at 0.4 mg/rat in the intracranial 9 L tumor model. The control group received CED infusion of saline.

As shown in Fig. 2, all animals in the control group expired due to tumor progression by day 21 and mean survival was only 16.5 days (median, 16.5 days). Systemic treatment with ACNU showed no improvement in survival. All animals expired by day 33 and mean survival was 19 days (median, 17 days). Animals treated with CED of ACNU at the dose of 0.005 mg/rat also expired by day 29 and mean survival was 18.2 days (median, 16.5 days). There was no significant advantage compared with the control group. Animals treated with CED of ACNU at the dose of 0.01 mg/rat expired by day 49 and mean survival was 26.5 days (median, 19.5 days). Although this CED treatment group showed a slight improvement in survival, there was no significant advantage compared with the group receiving i.v. administration of ACNU. Animals treated with CED of ACNU at the MTD of 0.02 mg/rat showed significantly improved survival rate compared with i.v. administration of ACNU ($p < 0.05$, log-rank test); treatment at the 0.02 mg/rat resulted in two of eight animals (25%) surviving beyond day 80 (median, 26.5 days).

Histopathologic evaluation of brain tissue was done in all animals at death or after sacrifice. Animals showing clinical signs of tumor progression were euthanized. Two animals survived to the study end at day 80, in the group receiving CED infusion of ACNU at the MTD (0.02 mg/rat), and showed complete pathologic responses (Fig. 3a). Tumor progression was observed in the brains of all rats, which died (Fig. 3b).

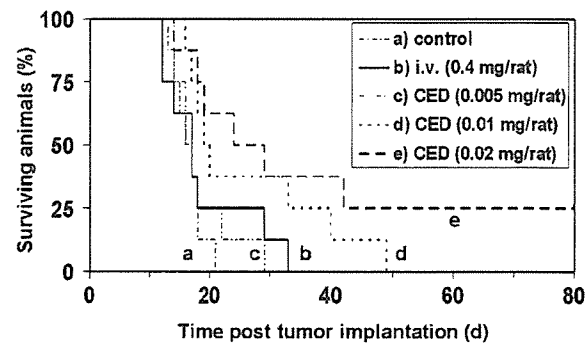

Fig. 2 Treatment of rats bearing 9 L tumors with CED or i.v. administration of ACNU. Seven days after tumor implantation within the brain, rats were treated with CED of saline (**a**), i.v. administration of ACNU at 0.4 mg/rat (**b**), and CED of ACNU at 0.005 mg/rat (**c**), 0.01 mg/rat (**d**), and 0.02 mg/rat (**e**). Eight animals per group

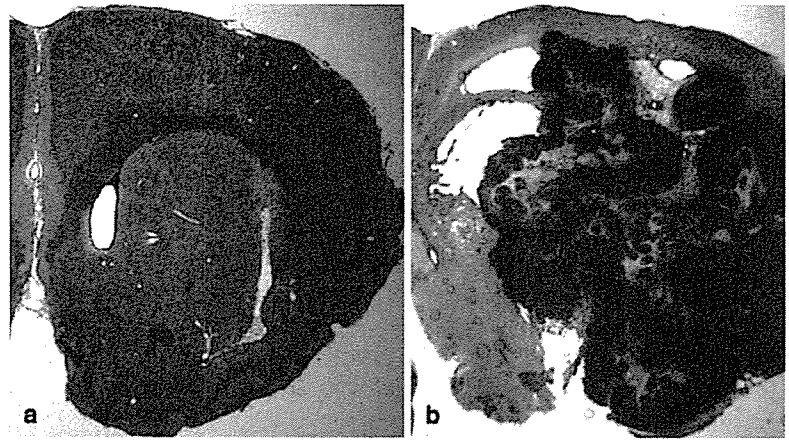

Fig. 3 Representative brain sections from surviving and non-surviving animals. (**a**) Brain section obtained from one of the survivors treated by CED of ACNU at 0.02 mg/rat. Neither survivor had residual tumor. (**b**) Brain section from a rat of the control group showing a typical tumor found in all non-surviving animals in which tumor progression led to death

Tissue concentration of ACNU following CED or intravenous administration

The mean tissue concentrations just after the treatment with CED of ACNU at the dose of 0.02 mg/rat, and i.v. injection of ACNU at 2.0 and 0.4 mg/rat were 3.21, 3.47, and 0.52 μg/g, respectively. CED of ACNU at the dose of 100-fold less total drug than i.v. injection carried an almost equivalent concentration of ACNU into rat brain tissue. The tissue concentration after treatment with CED at the dose of 0.02 mg/rat was almost as high as that of i.v. administration at the dose of 2.0 mg/rat, and was about six times as high as that of i.v. administration at the dose of 0.4 mg/rat. ACNU was completely cleared from the brain tissues within 4 h in all groups (Fig. 4).

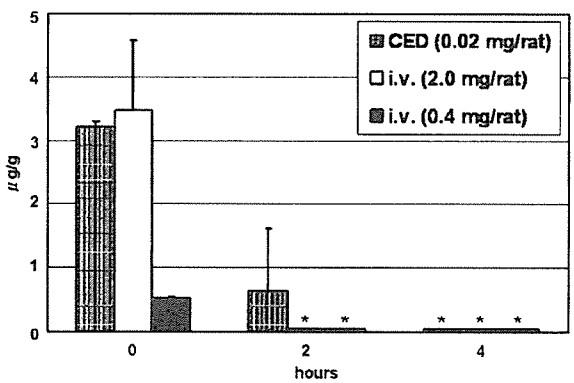

Fig. 4 Tissue concentrations of ACNU in the normal rat brain following single CED infusion and bolus i.v. injection. Drug concentrations were measured by high-performance liquid chromatography assay for ACNU. *: below the detection limit of 0.05 μ g/g

Discussion

Convection-enhanced delivery has shown considerable potential for the treatment of brain tumors, with some of the protocols now in clinical trials [5, 22]. ACNU is a hydrophilic nitrosourea with a proven efficacy against high-grade gliomas through systemic administration [18, 19]. Our studies demonstrated that combining ACNU with the CED technique provided safe and significant anti-tumor effects in animal brain tumor models.

To evaluate the safe dose of ACNU via CED, we performed the toxicity test in the normal brain parenchyma of intact rats. The established MTD was 0.02 mg/rat (1.0 mg/mL ACNU, 20 μL CED). This dose was far smaller than the clinically tolerable dose of 0.4 mg/rat for systemic administration, and CED at the dose of 0.02 mg/rat resulted in no systemic complication.

3-[(4-amino-2-methyl-5-pyrimidinyl) methyl]-1-(2-chloroethyl)-1-nitrosourea hydrochloride is lipophilic as well as hydrophilic under physiological conditions ($\log p = 0.92$). Hydrophilic ACNU delivered via CED is expected to distribute over the extracellular space of the brain, gradually becoming lipophilic, then taken up into the surrounding cells, and manifesting the anti-cancer effect.

As confirmed by high-performance liquid chromatography, ACNU administered via CED yielded much higher drug levels in brain tissue than i.v. administration. The survival study using 9 L rat brain tumor models revealed that CED infusion at the MTD of ACNU produced significantly improved survival rate compared with i.v. administration, and the anti-tumor effect of ACNU delivered via CED was dose-dependent. These results demonstrated that CED enhanced

the anti-tumor effect of hydrophilic ACNU compared with i.v. administration.

Infusion of a high concentration of ACNU resulted in increased local CNS toxicity, which was ascribed to the non-specific cytotoxicity of ACNU. The local neurotoxicity strictly limited the therapeutic window of ACNU delivered via CED, so we could not attempt dose escalation to increase the anti-tumor effect of ACNU. Several studies have utilized drug encapsulation in nano-particles to overcome such non-specific cytotoxicity of anticancer drugs [23–25]. Encapsulation of drugs increases tissue tolerance by reducing the acute tissue exposure and slowing the rate of drug release. Encapsulated ACNU in nano-particles may allow a higher dose of ACNU to be delivered via CED.

The short-tissue retention time of ACNU was another limiting factor of the anti-tumor efficacy in our study. ACNU infused via CED was completely cleared from the brain tissue within 4 h. Unencapsulated and water-soluble agents are typically cleared from the brain in less than one day [23, 24]. Furthermore, if the molecular weight of the agent is < 200–400, free exchange takes place between plasma and brain extracellular water across the BBB [15]. The rapid clearance of ACNU may be partially due to its small molecular weight (309.15). To extend the drug residence, encapsulation of drugs in nano-particles as described above is also possible. Encapsulated agents have prolonged tissue residence time in CED compared with free agents [23, 24]. Combining drug encapsulation techniques with CED may reduce CNS toxicity as well as increase tissue retention and anti-tumor efficacy.

The survival rate of animals treated with CED of ACNU at the dose of 0.02 mg/rat (0.1 mg/kg) was 25%. Presumably the difference between survivors and non-survivors within the same CED group could be attributed to the inhomogeneous drug distribution within the tumors. Heterogeneous distribution of anti-cancer drugs results in partial response and local recurrence of brain neoplasms [5, 26]. Current ongoing clinical CED lacks monitoring or confirmation of the drug distribution [5, 22], although several infusion sites can be selected to optimize catheter placement and achieve homogeneous drug distribution over the entire targeted lesion [5]. Further animal studies with CED are needed to improve the drug distribution in human brain tumors.

Several studies support the applicability of ACNU administered via CED to clinical treatment of high-grade gliomas in humans. Locally injected ACNU into recurrent gliomas was effective in inducing tumor necrosis and inhibiting tumor growth [27]. Intraventricular administration of ACNU is safe and efficacious in the treatment of malignant gliomas [28–30]. The present study also suggests that CED of ACNU is capable of increasing efficacy in the field of glioma treatment.

References

1. Stupp R, Mason WP, van den Bent MJ, Weller M, Fisher B, Taphoorn MJ, Belanger K, Brandes AA, Marosi C, Bogdahn U, Curschmann J, Janzer RC, Ludwin SK, Gorlia T, Allgeier A, Lacombe D, Cairncross JG, Eisenhauer E, Mirimanoff RO, European Organisation for Research, Treatment of Cancer Brain Tumor and Radiotherapy Groups, National Cancer Institute of Canada Clinical Trials Group (2005) Radiotherapy plus concomitant and adjuvant temozolomide for glioblastoma. N Engl J Med 352(10):987–996
2. Stewart LA (2002) Chemotherapy in adult high-grade glioma: a systematic review and meta-analysis of individual patient data from 12 randomised trials. Lancet 359:1011–1018
3. Groothuis DR (2000) The blood-brain and blood-tumor barriers: a review of strategies for increasing drug delivery. Neuro-oncol 2:45–59
4. Bobo RH, Laske DW, Akbasak A, Morrison PF, Dedrick RL, Oldfield EH (1994) Convection-enhanced delivery of macromolecules in the brain. Proc Natl Acad Sci USA 91:2076–2080
5. Vogelbaum MA (2005) Convection enhanced delivery for the treatment of malignant gliomas: symposium review. J Neurooncol 73:57–69
6. Mahaley MS Jr (1991) Neuro-oncology index and review (adult primary brain tumors). Radiotherapy, chemotherapy, immunotherapy, photodynamic therapy. J Neurooncol 11:85–147
7. Gilmann AG, Goodman LS, Rall TW, Murad TW (eds) (1985) Goodman and Gilman's the pharmacological basis of therapeutics, 7th edn. Macmillan, New York, pp 1260–1261
8. Walter KA, Tamargo RJ, Olivi A, Burger PC, Brem H (1995) Intratumoral chemotherapy. Neurosurgery 37:1128–1145
9. Brem H, Piantadosi S, Burger PC, Walker M, Selker R, Vick NA, Black K, Sisti M, Brem S, Mohr G, Muller P, Morawetz R, Schold SC (1995) Placebo-controlled trial of safety and efficacy of intraoperative controlled delivery by biodegradable polymers of chemotherapy for recurrent gliomas. Lancet 345:1008–1012
10. Westphal M, Hilt DC, Bortey E, Delavault P, Olivares R, Warnke PC, Whittle IR, Jaaskelainen J, Ram Z (2003) A phase 3 trial of local chemotherapy with biodegradable carmustine (BCNU) wafers (Gliadel wafers) in patients with primary malignant glioma. Neuro-oncol 5:79–88
11. Saito R, Krauze MT, Noble CO, Tamas M, Drummond DC, Kirpotin DB, Berger MS, Park JW, Bankiewicz KS (2006) Tissue affinity of the infusate affects the distribution volume during convection-enhanced delivery into rodent brains: Implications for local drug delivery. J Neurosci Methods 9:S0165–S0270
12. Buahin KG, Brem H (1995) Interstitial chemotherapy of experimental brain tumors: comparison of intratumoral injection versus polymeric controlled release. J Neurooncol 26:103–110
13. Fleming AB, Saltzman WM (2002) Pharmacokinetics of the carmustine implant. Clin Pharmacokinet 41:403–419
14. Bruce JN, Falavigna A, Johnson JP, Hall JS, Birch BD, Yoon JT, Wu EX, Fine RL, Parsa AT (2000) Intracerebral clysis in a rat glioma model. Neurosurgery 46:683–691

15. Walker MD, Hilton J (1976) Nitrosourea pharmacodynamics in relation to the central nervous system. Cancer Treat Rep 60:725–728
16. Hansch C, Smith N, Engle R, Wood H (1972) Quantitative structure-activity relationships of antineoplastic drugs: nitrosoureas and triazenoimidazoles. Cancer Chemother Rep 56:443–456
17. Mori T, Mineura K, Katakura R (1979) Chemotherapy of malignant brain tumor by a water-soluble anti-tumor nitrosourea, ACNU. Neurol Med Chir (Tokyo) 19:1157–1171
18. Takakura K, Abe H, Tanaka R, Kitamura K, Miwa T, Takeuchi K, Yamamoto S, Kageyama N, Handa H, Mogami H et al (1986) Effects of ACNU and radiotherapy on malignant glioma. J Neurosurg 64:53–57
19. Weller M, Muller B, Koch R, Bamberg M, Krauseneck P, Neuro-Oncology Working Group of the German Cancer Society (2003) Neuro-oncology Working Group 01 trial of nimustine plus teniposide versus nimustine plus cytarabine chemotherapy in addition to involved-field radiotherapy in the first-line treatment of malignant glioma. J Clin Oncol 21:3276–3284
20. Saito R, Bringas JR, McKnight TR, Wendland MF, Mamot C, Drummond DC, Kirpotin DB, Park JW, Berger MS, Bankiewicz KS (2004) Distribution of liposomes into brain and rat brain tumor models by convection-enhanced delivery monitored with magnetic resonance imaging. Cancer Res 64:2572–2579
21. Krauze MT, Saito R, Noble C, Tamas M, Bringas J, Park JW, Berger MS, Bankiewicz K (2005) Reflux-free cannula for convection-enhanced high-speed delivery of therapeutic agents. J Neurosurg 103:923–929
22. Kunwar S (2003) Convection enhanced delivery of IL13-PE38QQR for treatment of recurrent malignant glioma: presentation of interim findings from ongoing phase 1 studies. Acta Neurochir Suppl 88:105–111
23. Noble CO, Krauze MT, Drummond DC, Yamashita Y, Saito R, Berger MS, Kirpotin DB, Bankiewicz KS, Park JW (2006) Novel nanoliposomal CPT-11 infused by convection-enhanced delivery in intracranial tumors: pharmacology and efficacy. Cancer Res 66:2801–2806
24. Saito R, Krauze MT, Noble CO, Drummond DC, Kirpotin DB, Berger MS, Park JW, Bankiewicz KS (2006) Convection-enhanced delivery of Ls-TPT enables an effective, continuous, low-dose chemotherapy against malignant glioma xenograft model. Neuro-oncol 24:S1522–S8517
25. Yamashita Y, Saito R, Krauze MT, Kawaguchi T, Noble CO, Drummond DC, Kirpotin DB, Berger MS, Park JW, Berger MS, Bankiewicz KS (2006) Convection-enhanced delivery of liposomal doxorubicin in intracranial brain tumor xenografts. Targeted Oncol 1:79–85
26. Vavra M, Ali MJ, Kang EW, Navalitloha Y, Ebert A, Allen CV, Groothuis DR (2004) Comparative pharmacokinetics of 14C-sucrose in RG-2 rat gliomas after intravenous and convection-enhanced delivery. Neuro-oncol 6:104–112
27. Wakabayashi T, Yoshida J, Mizuno M, Kajita Y (2001) Intratumoral microinfusion of nimustine (ACNU) for recurrent glioma. Brain Tumor Pathol 18:23–28
28. Levin VA, Byrd D, Campbell J, Giannini DD, Borcich JK, Davis RL (1985) Central nervous system toxicity and cerebrospinal fluid pharmacokinetics of intraventricular 3-[(4-amino-2-methyl-5-pyrimidinyl)ethyl]-1-(2-chloroethyl)-1-nitro soureas and other nitrosoureas in beagles. Cancer Res 45:3803–3809
29. Ushio Y, Kochi M, Kitamura I, Kuratsu J (1998) Ventriculolumber perfusion of 3-[(4-amino-2-methyl-5-pyrimidinyl)-methyl]-1-(2-chloroethyl-1-nitrosourea hydrochloride for subarachnoid dissemination of gliomas. J Neurooncol 38:207–212
30. Kochi M, Kuratsu J, Mihara Y, Takaki S, Seto H, Uemura S, Ushio Y (1993) Ventriculolumbar perfusion of 3-[(4-amino-2-methyl-5-pyrimidinyl)methyl]-1-(2-chloroethyl)-1-nitrosourea hydrochloride. Neurosurgery 33:817–823

J Neurosurg 106:263–269, 2007

Ischemic complications associated with resection of opercular glioma

TOSHIHIRO KUMABE, M.D.,[1] SHUICHI HIGANO, M.D.,[2] SHOKI TAKAHASHI, M.D.,[2] AND TEIJI TOMINAGA, M.D.[1]

Departments of [1]Neurosurgery and [2]Diagnostic Radiology, Tohoku University Graduate School of Medicine, Sendai, Japan

Object. Opercular glioma inferolateral to the hand/digit sensorimotor area can be resected safely using a neuronavigation system and functional brain mapping techniques. However, the surgery can still sometimes cause postoperative ischemic complications, the character of which remains unclear. The authors of this study investigated the occurrence of infarction associated with resection of opercular glioma and the arterial supply to this region.

Methods. The study involved 11 consecutive patients with gliomas located in the opercular region around the orofacial primary motor and somatosensory cortices but not involving either the hand/digit area or the insula, who had been treated in their department after 1997. Both pre- and postoperative diffusion-weighted magnetic resonance (MR) imaging was performed in the nine consecutive patients after 1998 to detect ischemic complications. All patients underwent open surgery for maximum tumor resection. Postoperative MR imaging identified infarction beneath the resection cavity in all patients. Permanent motor deficits associated with infarction involving the descending motor pathway developed in two patients. Cadaveric angiography showed that the distributing arteries to the corona radiata were the long insular arteries and/or medullary arteries from the opercular and cortical segments of the middle cerebral artery.

Conclusions. Subcortical resection around the upper limiting sulcus of the posterior region of the insula and wide resection in the anteroposterior and cephalocaudal directions of the opercular region were considered to be risk factors of the critical infarction. Surgeons should be aware that resection of opercular glioma can disrupt the blood supply of the corona radiata, and carries the risk of permanent motor deficits.

KEY WORDS • **infarction** • **complication** • **glioma** • **descending motor pathway** • **operculum** • **diffusion-weighted imaging**

PRECISE localization of a glioma in the frontoparietal opercular region inferolateral to the hand/digit sensorimotor area is now possible using various methods including functional brain mapping techniques, neuronavigation systems, intraoperative MR imaging, and photodynamic diagnosis using various photosensitizers. Therefore, gliomas in this location, even in the dominant hemisphere, can be totally resected without causing permanent neurological deficits.[5,9,11,12] During such procedures, surgical techniques for opercular glioma have concentrated on the identification and preservation of the cortical and subcortical functions.[5,11,12] However, little is known about the ischemic complications that can occur after the resection of an opercular glioma.

Diffusion-weighted MR imaging, which reflects the degree of water diffusion in vivo, is an invaluable tool for the diagnosis of acute stroke and other types of brain injury.[14] Several potential applications of DW MR imaging in patients with gliomas have been recently investigated, mainly for the evaluation of tumor cellularity.[7,8,16,21] Recently, postoperative DW MR imaging has been proposed as a routine study to identify ischemic complications after resection of the glioma.[15] Diffusion-weighted MR imaging detected abnormalities after resection in approximately two thirds of newly diagnosed gliomas. At our institution, postoperative MR imaging including DW imaging has been performed for nearly 10 years as one of the examinations used to determine the postoperative state of patients after tumor removal and has disclosed evidence of postoperative ischemic complications.

In the present study we investigated the postoperative ischemic complications and DW MR imaging findings in 11 patients with pure opercular gliomas surgically treated during the past 9 years. Microangiography studies of cadavers were also analyzed to identify the blood supply for the corona radiata. Finally, referring to the results of the microangiographic analysis, we tried to determine the risk factors for critical infarction at the corona radiata that were likely to result in permanent motor deficits.

Abbreviations used in this paper: DW = diffusion-weighted; GBM = glioblastoma multiforme; MCA = middle cerebral artery; MR = magnetic resonance.

TABLE 1

*Summary of characteristics in 11 cases of opercular glioma**

Case No.	Age (yrs), Sex	Diagnosis	WHO Grade	Tumor Location	Dominant Hemisphere	Presenting Symptoms	Date of Surgery	State of Anesthesia
1	26, M	A	II	rt face motor area	no	lt facial seizure followed by generalized convulsion	1/23/97	awake
2	31, M	AA	III	lt face/tongue motor area	yes	generalized convulsion	9/11/97	awake
3	68, M	AA	III	rt tongue sensorimotor area	no	lt facial seizure	1/27/98	awake
4	3, M	DNET	I	rt face motor area	no	lt facial seizure	12/16/99	general
5	38, M	AA	III	lt face motor area	yes	lt facial seizure	2/28/00	general
6	69, F	GBM	IV	rt face/tongue sensorimotor area	no	lt facial seizure followed by lt hemiconvulsion	1/24/02	general
7	49, M	OA	II	rt tongue sensorimotor area	no	incidental	2/5/02	general
8	21, M	A	II	lt tongue sensorimotor area	no	rt facial seizure followed by generalized convulsion	4/11/02	general
9	38, M	AA	III	rt face motor area	no	lt facial seizure	7/22/02	general
10	34, F	O	II	lt face/tongue motor area	yes	rt facial seizure	4/28/03	awake
11	23, M	AA	III	lt face motor area	yes	loss of consciousness	6/9/05	awake

* A = astrocytoma; AA = anaplastic astrocytoma; DCS = direct cortical stimulation; DNET = dysembryoplastic neuroepithelial tumor; KPS = Karnofsky Performance Scale; O = oligodendroglioma; OA = oligoastrocytoma; SCS = subcortical stimulation; US = ultrasonography; WHO = World Health Organization.

Clinical Material and Methods

Patient Population and Tumor Characteristics

This study included 11 consecutive patients, nine males and two females with ages from 3 to 69 years (mean 36.4 ± 19.8 years). Each patient harbored a newly diagnosed glioma located at the opercular region around the orofacial primary motor and somatosensory cortices but not involving either the hand/digit area or the insula and treated in our department after 1997. The tumors included one dysembryoplastic neuroepithelial tumor, two astrocytomas, one oligoastrocytoma, one oligodendroglioma, five anaplastic astrocytomas, and one GBM. Patient characteristics are summarized in Table 1. Informed consent for this study was obtained from all the patients, and institutional review board approval was waived because of the retrospective nature of the study.

Surgical Procedure and Intraoperative Neurophysiological Monitoring

All patients underwent open surgery for maximum tumor resection. Cortical mapping was performed in eight patients, using electric stimuli of 3 to 12 mA to identify the sensorimotor and language cortices, according to a method described previously.[1–4] Five patients were treated while in an awake condition. Primary speech cortex was identified based on speech arrest or hesitation due to stimulation during counting or object naming by the patient. A frameless stereotactic navigation device (ISG Viewing Wand, ISG Technologies; ViewScope, Elekta IGS; or Vector Vision, BrainLAB) was used in all nine cases after 1998; ultrasonography was used in the initial two cases.

Tumor resection was performed using an Ultrasonic Surgical Aspirator (Sonopet, Miwatec Co., Ltd.). All of the opercular arteries were carefully dissected and preserved. If the tumor infiltrated down to the sylvian fissure, thorough dissection of the affected sylvian fissure was initially performed to identify and preserve the insular and opercular segments of the MCAs.

Only the minimum amount of Surgicel (Ethicon, Inc.) was routinely used for hemostasis. Dexamethasone (4 mg) was given every 6 hours with varied tapering schedules, and the administration of anticonvulsants (typically phenytoin and/or zonisamide) and antibiotics was begun or continued in patients during the immediate postoperative period.

Neuroimaging Studies

All patients underwent preoperative, postoperative, and subsequent follow-up MR imaging at our department. Postoperative imaging was performed within 72 hours of surgery. Data from pre- and postoperative DW MR imaging were available for the nine consecutive patients treated after 1998.

For MR imaging, we used a 1.5-tesla system (Signa Horizon LX CV/i, GE Medical Systems) with a conventional quadrature head coil. We obtained T_1-weighted images before and after Gd administration, T_2-weighted images, and DW images during the same imaging session without repositioning the patient's head. Axial DW images were obtained using fat-suppressed spin echo–echo planar imaging (TR 5000 msec, TE 72 msec, number of excitations 2, slice thickness 6 mm, gap 2 mm, matrix 128 × 128, and field of view 23 × 23 cm) with three orthogonal directional motion-probing gradients (b = 1000 seconds/mm^2), followed by automatic generation of isotropic DW images. To evaluate the

TABLE 1
(continued)

Stimulation	Navigation System	Extent of Resection	DW Image	Immediate Postop Outcome	Long-Term Deficit	Follow Up (3/26/06)
DCS	US	total	not examined	lt facial palsy	none	no recurrence, KPS 100
DCS	US	total	not examined	rt facial palsy, dysarthria	slight dysarthria	no recurrence, KPS 90
DCS	viewing wand	total	infarction beneath resection cavity	lt hemiparesis	lt fine movement disorder	dead 5/14/99 (dissemination)
none	ViewScope	total	infarction beneath resection cavity	lt hemiparesis	none	no recurrence, KPS 100
DCS & SCS	ViewScope	total	infarction beneath resection cavity	rt facial palsy, dysarthria	slight dysarthria	no recurrence, KPS 90
DCS & SCS	ViewScope	subtotal	infarction beneath resection cavity	lt hemiparesis	lt hemiparesis	dead 4/28/04 (local recurrence & dissemination)
none	ViewScope	total	infarction beneath resection cavity	lt facial palsy	none	no recurrence, KPS 100
none	ViewScope	total	infarction beneath resection cavity	none	none	no recurrence, KPS 100
DCS & SCS	ViewScope	total	infarction beneath resection cavity	none	none	no recurrence, KPS 100
DCS & SCS	ViewScope	subtotal	infarction beneath resection cavity	rt facial palsy, dysarthria	dysarthria	no recurrence, KPS 90
DCS & SCS	Vector Vision	subtotal	infarction beneath resection cavity	rt fine movement disorder, dysarthria	none	no recurrence, KPS 100

spatial relationship between the postoperative ischemic lesion and the pyramidal tract, coronal DW images were also obtained using similar conditions, but the motion-probing gradient was applied in only the anteroposterior direction. The pyramidal tracts, which run in the cephalocaudal direction, were delineated as slightly hyperintense to adjacent brain parenchyma in these coronal images.

The extent of the resection was evaluated according to MR images obtained within 72 hours of surgery. If the tumor had been enhanced on the preoperative MR images, its gross-total resection was defined as no residual enhanced tumor, its subtotal resection as more than 75% removal, and its partial resection as less than 75% removal. If the tumor had not been enhanced on the preoperative MR images, resection was evaluated based on the presence of residual high-intensity lesion on the T_2-weighted MR images.

Postoperative Neurological Outcomes

The postoperative neurological outcome was recorded and confirmed by retrospective review of all hospital records and physician notes. Immediate postoperative neurological function was determined during the first 7 days after surgery, and long-term function was determined between 3 and 6 months after surgery.

Microangiographic Analysis of Vascular Supply to the Corona Radiata

Coronal and axial microangiograms of five cadaveric brains without gross brain pathological features, which were part of a microangiographic study on the distribution of the basal perforating arteries that had been conducted by one of the authors (S.T.) in 1985,[17,18] were reanalyzed to examine pial cortical arteries in and around the insuloopercular region and to identify the blood supply to the corona radiata.

Results

Extent of Resection

Table 1 outlines the extent of resection in each case, as determined by quantitative volumetric analysis using postoperative MR imaging. Gross-total resection of the lesions was accomplished in eight patients (Cases 1–5 and 7–9). Subtotal resection was achieved in three patients (Cases 6, 10, and 11).

Postoperative MR Imaging and Neurological Outcomes

Postoperative DW MR images showed markedly hyperintense areas representing restricted diffusion in all nine patients treated after 1998. These lesions were all contiguous with the resection cavity. The size of the lesions beneath the resection cavity varied from case to case. All lesions appeared as high-intensity areas on T_2-weighted MR images. Similar high-intensity lesions were also depicted on postoperative T_2-weighted images in the two initial patients without DW imaging data.

Details on postoperative neurological deficits are shown in Table 1. Eight patients, all of whom had undergone relatively small areas of resection mostly located in the face motor area, did not suffer impairment of long-tract function after surgery; three patients (Cases 3, 4, and 6) did have impaired long-tract function immediately after surgery. The lesions with restricted diffusion involved the descending motor pathway in these three patients. Tumor was located in the orofacial sensorimotor area in two of these patients

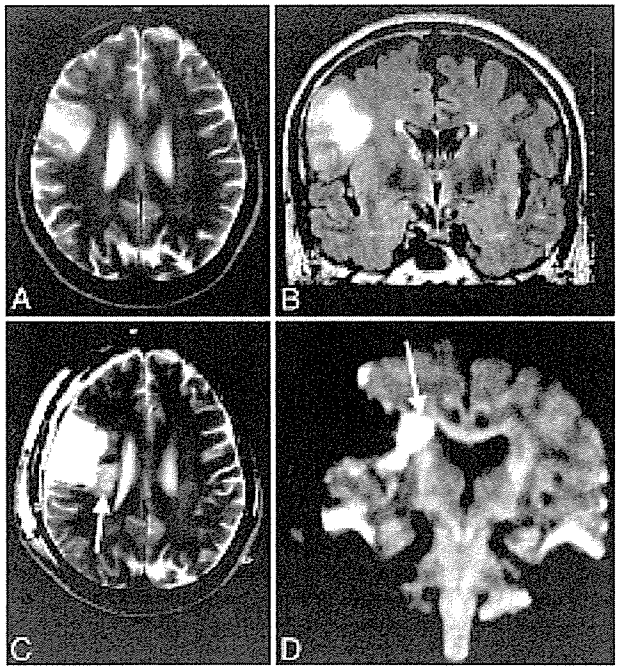

FIG. 1. Case 3. Images obtained in a 68-year-old man with an anaplastic astrocytoma in the right tongue sensorimotor area. Preoperative axial T_2-weighted (A) and coronal fluid-attenuated inversion-recovery (B) MR images revealing a high-intensity mass in the right frontoparietal opercular region. Postoperative axial T_2-weighted (C) and coronal DW (D) MR images showing total removal of the tumor and a new high-intensity lesion *(arrows)* beneath the resection cavity. The lesion extends to the region of the corona radiata, probably involving the corticospinal tract. This tract appears as a bandlike area of slightly high intensity on the coronal DW image with the motion-probing gradient applied only in the anteroposterior direction.

(Cases 3 and 6). A relatively small resection in these two patients was performed around the white matter above the upper limiting sulcus of the posterior region of the insula, and wide resection was undertaken in the anteroposterior and cephalocaudal directions of the opercular region (Figs. 1–4).

Microangiographic Analysis of Vascular Supply to the Corona Radiata

Coronal microangiography of the cadavers showed that the corona radiata is constantly supplied by the lateral striate arteries, the long insular arteries originating from insular portions of the MCA, and the medullary arteries from the opercular and cortical portions of the MCA (Fig. 5). Surgical removal for opercular glioma, even if not involving the insula, could compromise the latter two fine arteries, resulting in cerebral infarction at the corona radiata.

Illustrative Cases

Case 3

History and Examination. This 68-year-old man presented with an anaplastic astrocytoma manifesting as left facial seizures. Results of T_2-weighted MR imaging demonstrated a hyperintense lesion in the right opercular portions of the inferior frontal, precentral, and postcentral gyri inferolateral to the precentral knob, not involving the insula (Fig. 1A). Administration of a contrast medium caused no enhancement. Neurological and neuropsychological examination revealed no abnormality.

Operation. A right frontoparietotemporal craniotomy was performed with the patient in an awake condition. Direct cortical stimulation identified the face motor area and the primary sensory sites of the tongue and face. The sylvian fissure was thoroughly dissected toward the distal end, and the insular surface was exposed under the operating microscope. The precentral and central arteries were separated from the tumor and preserved. The lesion was totally removed up to the face motor area and toward the deepest portion using the upper limiting sulcus as the anatomical landmark and the ISG Viewing Wand (Fig. 2).

Postoperative Course. Almost complete left hemiparesis was observed postoperatively. Magnetic resonance images showed that the entire lesion had been resected but revealed an ischemic area beneath the resection cavity involving the descending motor pathway (Fig. 1B). As adjuvant therapy, the patient received 72 Gy hyperfractionated radiation to the extended local field. His left hemiparesis resolved except

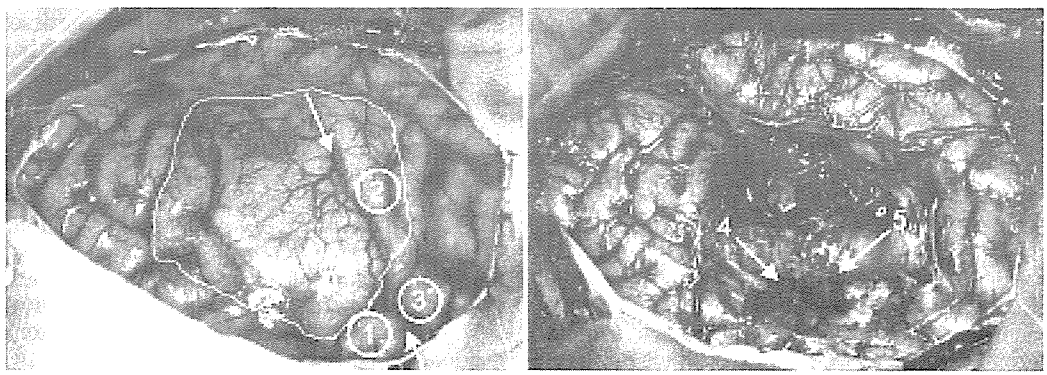

FIG. 2. Case 3. Intraoperative photographs obtained before *(left)* and after *(right)* tumor resection. *Left:* Note the results of functional brain mapping: 1, face motor; 2, tongue sensory; and 3, face sensory. The outline indicates the location of the tumor; the *arrows* represent the central sulcus. *Right:* Note preservation of the precentral (4) and central (5) arteries.

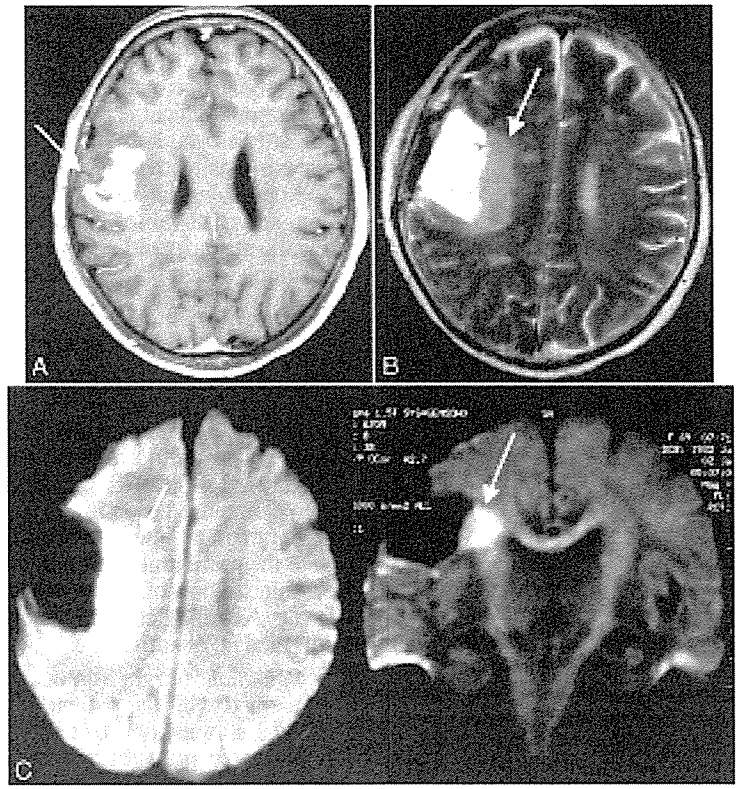

FIG. 3. Case 6. Images obtained in a 69-year-old woman with a right frontoparietal GBM. A: Preoperative axial Gd-enhanced T_1-weighted MR image demonstrating an irregularly enhanced mass lesion in the opercular region around the central sulcus *(arrow)*. B: Postoperative axial T_2-weighted MR image depicting total removal of the tumor and a new lesion of high intensity *(arrow)* beneath the resection cavity. C: Postoperative axial *(left)* and coronal *(right)* DW MR images revealing the new lesion *(arrows)* beneath the resection cavity with reduced diffusion probably involving the corticospinal tract.

for impaired fine movement of the left finger. He was discharged home and able to ambulate 2 months postsurgery.

Case 6

History and Examination. This 69-year-old woman presented with a GBM manifesting as left facial seizures followed by left hemiconvulsion. Preoperative T_1-weighted MR images with contrast medium exhibited an enhanced mass in the right opercular portions of the inferior frontal, precentral, and postcentral gyri inferolateral to the precentral knob, not involving the insula (Fig. 3A). Neurological and neuropsychological examination revealed no abnormality.

Operation. A right frontoparietotemporal craniotomy was performed with the patient in a state of general anesthesia. Direct cortical stimulation identified the hand/digit motor area. The sylvian fissure was thoroughly dissected toward the distal end, and the insular surface was exposed under the operating microscope. The precentral, central, and anterior parietal arteries were separated from the tumor and preserved. The lower portion of the lesion was resected toward the deepest portion by using the upper limiting sulcus as the anatomical landmark and the ViewScope. The tumor was removed in a stepwise manner while monitoring the muscle contraction by direct cortical stimulation to the hand/digit motor area (Fig. 4). The positive cortical response gradually became duller at the end of the surgery.

Postoperative Course. Almost complete left hemiparesis was observed postoperatively. Magnetic resonance images obtained after surgery showed that most of the enhanced lesion had been resected, but an ischemic area was found beneath the resection cavity involving the descending motor pathway (Fig. 3B and C). The patient's left hemiparesis did not resolve.

Discussion

Surgical removal of glioma in the opercular region presents many challenges. In 1991, LeRoux et al.[11] first reported that gliomas involving the nondominant face motor cortex can be safely removed using brain mapping techniques to localize the rolandic cortex and avoid resection of the hand motor cortex and descending subcortical motor pathways. However, resection of the face motor cortex in the dominant hemisphere was not recommended because language localization in the cortical zones is contiguous with this region. In 1995, Ebeling and Kothbauer[5] supposed that radical tumor resection of a purely opercular glioma, not including the insula, in the dominant hemisphere can be

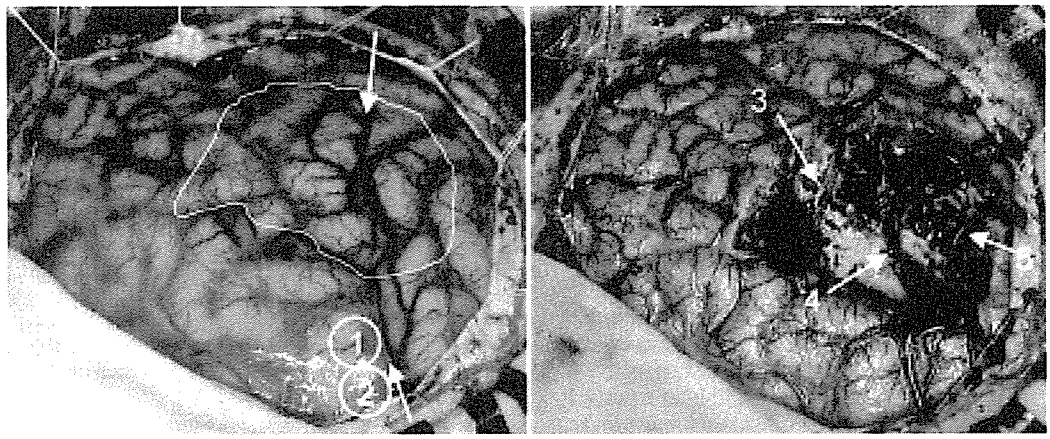

FIG. 4. Case 6. Intraoperative photographs obtained before *(left)* and after *(right)* tumor resection. *Left:* Note the results of functional brain mapping: 1 and 2, hand/digit motor. The *outline* indicates the tumor location; the *arrows* represent the central sulcus. *Right:* Note preservation of the precentral (3), central (4), and anterior parietal (5) arteries.

achieved without significant lasting morbidity. However, only biopsy was recommended for large dominant insular or opercular–insular tumors, because the lenticulostriate arteries hinder total resection and no clear border toward the internal capsule can be found. In 2004, Peraud et al.[12] reported the surgical results of 14 cases of opercular gliomas, stressing the importance of intraoperative neuromonitoring as an aid to surgery in the dominant opercular region. The severity and duration of postoperative deficits was well correlated with the distance from the resection margin to the next positive stimulation point(s), and a distance of more than 5 mm was found to avoid major impairments. Clearly, intraoperative functional brain mapping techniques can help preserve cortical and subcortical functions. However, vascular damage during resection of opercular glioma remains less well understood.

Recently, restricted diffusion abnormalities were found adjacent to the resection cavity on immediately postoperative images in 64% of cases.[15] Both cortical and subcortical lesions with restricted diffusion were observed after surgery. In the present study, postoperative MR images including DW images disclosed infarcted lesions in all patients, and these lesions unexpectedly extended to the descending motor pathway in the corona radiata in three patients, which could have resulted in the impairment of long-tract function. These infarcted lesions were probably caused by disruption of the blood supply during the surgical procedures.

Microangiographic analysis in this study revealed that the corona radiata is supplied by the lateral striate arteries, long insular arteries, and medullary arteries from the opercular and cortical segments of the MCA passing over the frontoparietal operculum. According to the study data collected by Ture et al.,[20] approximately 85 to 90% of insular arteries are short and supply the insular cortex and extreme capsule, 10% are medium length and supply the claustrum and external capsule, and 3 to 5% are long and extend as far

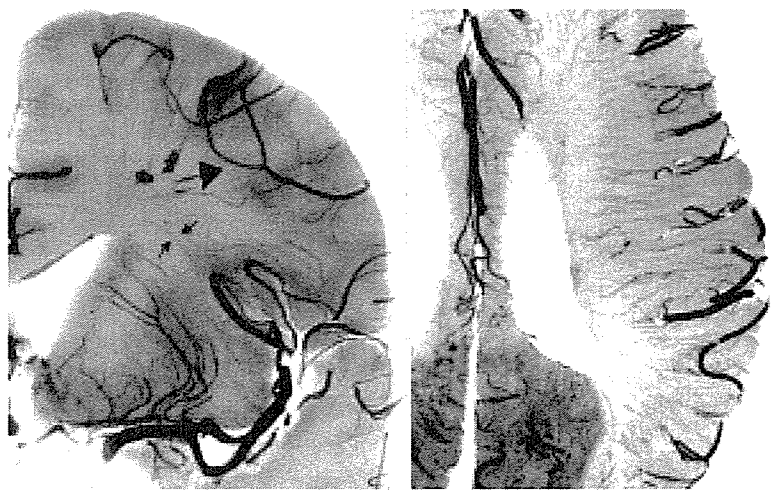

FIG. 5. Coronal *(left)* and axial *(right)* microangiograms of a cadaveric brain slice through the interventricular foramina. Both long insular arteries *(arrows)* arising from the insular portions of the MCA and the medullary arteries *(arrowhead)* from the opercular and cortical portions of the MCA course toward the ventricular wall and supply the region of the corona radiata.

as the corona radiata. Interruption of blood flow to these long insular arteries during the resection of intrinsic insular tumor may result in hemiparesis; thus, these arteries should be preserved to prevent infarction of the corona radiata.[6,10,19,20]

Data in the present study demonstrated that, in addition to the long insular arteries, the long medullary arteries from the opercular and cortical segments of the MCA passing over the frontoparietal operculum contribute to the arterial supply to the corona radiata. Although the vascular supply can show individual variations, these long medullary arteries can be impaired during the resection of a pure opercular glioma. Adequate collateral blood supply would not be expected[13] because intraparenchymal arterioles such as the lateral striate arteries, long insular arteries, and long medullary arteries are all end arteries without substantial anastomoses with other arteries except in pathological cases like moyamoya disease. If the impaired arteries supply most of the descending motor pathway, resection of opercular glioma is likely to result in hemiparesis.

The long insular arteries are mostly located in the posterior region of the insula,[20] most commonly on the posterior half of the central insular sulcus and on the long gyri.[19] Thus, subcortical resection around the upper limiting sulcus of the posterior region of the insula carries a higher risk of sacrifice of the long insular arteries, which may lead to extensive corona radiata infarction, and ultimately critical damage to the descending motor pathway. Similarly, a wide resection in the anteroposterior and cephalocaudal directions of the opercular region could damage a large number of medullary arteries from the opercular and cortical segments of the MCA over the frontoparietal operculum. In our experience, these two maneuvers appeared to be risk factors for critical infarction in the corona radiata after resection of an opercular glioma. However, reliable methods for avoiding damage to the long insular and medullary arteries are not available. Limited resection of the operculum as well as sparing of the posterior region of the insula may be the only measures presently available to avoid injury to a large number of long insular arteries and long medullary arteries. The development of new surgical devices to remove an opercular glioma with preservation of thin blood vessels like these arteries is to be expected in the future.

Conclusions

In the present study we found that ischemic complications occurring beneath the resection cavity including the pyramidal tract within the corona radiata are caused by damage to the distributing arteries—in particular, the long insular arteries and/or medullary arteries from the opercular and cortical segments of the MCA passing over the frontoparietal operculum—after resection of glioma in the frontoparietal opercular region inferolateral to the hand/digit sensorimotor area. Surgeons should be aware of the risk of ischemic complications during resection of opercular glioma and the possibility of permanent motor deficits.

References

1. Berger MS: Malignant astrocytomas: surgical aspects. **Semin Oncol 21:**172–185, 1994
2. Berger MS, Deliganis AV, Dobbins J, Keles GE: The effect of extent of resection on recurrence in patients with low grade cerebral hemisphere gliomas. **Cancer 74:**1784–1791, 1994
3. Berger MS, Kincaid J, Ojemann GA, Lettich E: Brain mapping techniques to maximize resection, safety, and seizure control in children with brain tumors. **Neurosurgery 25:**786–792, 1989
4. Berger MS, Ojemann GA, Lettich E: Neurophysiological monitoring during astrocytoma surgery. **Neurosurg Clin N Am 1:** 65–80, 1990
5. Ebeling U, Kothbauer K: Circumscribed low grade astrocytomas in the dominant opercular and insular region: a pilot study. **Acta Neurochir 132:**66–74, 1995
6. Hentschel SJ, Lang FF: Surgical resection of intrinsic insular tumors. **Neurosurgery 57 (1 Suppl):**176–183, 2005
7. Higano S, Yun X, Kumabe T, Watanabe M, Mugikura S, Umetsu A, et al: Malignant astrocytic tumors: clinical importance of apparent diffusion coefficient in prediction of grade and prognosis. **Radiology 241:**839–846, 2006
8. Kitis O, Altay H, Calli C, Yunten N, Akalin T, Yurtseven T: Minimum apparent diffusion coefficients in the evaluation of brain tumors. **Eur J Radiol 55:**393–400, 2005
9. Kumabe T, Nakasato N, Suzuki K, Sato K, Sonoda Y, Kawagishi J, et al: Two-staged resection of a left frontal astrocytoma involving the operculum and insula using intraoperative neurophysiological monitoring—case report. **Neurol Med Chir 38:**503–507, 1998
10. Lang FF, Olansen NE, DeMonte F, Gokaslan ZL, Holland EC, Kalhorn C, et al: Surgical resection of intrinsic insular tumors: complication avoidance. **J Neurosurg 95:**638–650, 2001
11. LeRoux PD, Berger MS, Haglund MM, Pilcher WH, Ojemann GA: Resection of intrinsic tumors from nondominant face motor cortex using stimulation mapping: report of two cases. **Surg Neurol 36:**44–48, 1991
12. Peraud A, Ilmberger J, Reulen HJ: Surgical resection of gliomas WHO grade II and III located in the opercular region. **Acta Neurochir 146:**9–18, 2004
13. Phan TG, Donnan GA, Wright PM, Reutens DC: A digital map of middle cerebral artery infarcts associated with middle cerebral artery trunk and branch occlusion. **Stroke 36:**986–991, 2005
14. Schaefer PW, Grant PE, Gonzalez RG: Diffusion-weighted MR imaging of the brain. **Radiology 217:**331–345, 2000
15. Smith JS, Cha S, Mayo MC, McDermott MW, Parsa AT, Chang SM, et al: Serial diffusion-weighted magnetic resonance imaging in cases of glioma: distinguishing tumor recurrence from postresection injury. **J Neurosurg 103:**428–438, 2005
16. Sugahara T, Korogi Y, Kochi M, Ikushima I, Shigematu Y, Hirai T, et al: Usefulness of diffusion-weighted MRI with echo-planar technique in the evaluation of cellularity in gliomas. **J Magn Reson Imaging 9:**53–60, 1999
17. Takahashi S, Goto K, Fukasawa H, Kawata Y, Uemura K, Suzuki K: Computed tomography of cerebral infarction along the distribution of the basal perforating arteries. Part I: Striate arterial group. **Radiology 155:**107–118, 1985
18. Takahashi S, Goto K, Fukasawa H, Kawata Y, Uemura K, Yaguchi K: Computed tomography of cerebral infarction along the distribution of the basal perforating arteries. Part II: Thalamic arterial group. **Radiology 155:**119–130, 1985
19. Tanriover N, Rhoton AL Jr, Kawashima M, Ulm AJ, Yasuda A: Microsurgical anatomy of the insula and the sylvian fissure. **J Neurosurg 100:**891–922, 2004
20. Ture U, Yaşargil MG, Al-Mefty O, Yaşargil DC: Arteries of the insula. **J Neurosurg 92:**676–687, 2000
21. Zimmerman RD: Is there a role for diffusion-weighted imaging in patients with brain tumors or is the "bloom off the rose"? **AJNR 22:**1013–1014, 2001

Manuscript submitted March 26, 2006.
Accepted August 7, 2006.

Address reprint requests to: Toshihiro Kumabe, M.D., Department of Neurosurgery, Tohoku University Graduate School of Medicine, 1–1 Seiryo-machi, Aoba-ku, Sendai 980–8574, Japan. email: kuma@nsg.med.tohoku.ac.jp.

No Shinkei Geka, 34(1): 73-81, 2005

症例 ◆ Case Report

脈絡叢乳頭腫/乳頭癌7例の検討*

野下 展生[1)] 隈部 俊宏[1)] 嘉山 孝正[2)] 冨永 悌二[1)]

Choroid Plexus Tumors : Report of 7 Cases in a Single Institution

Nobuo NOSHITA[1)], Toshihiro KUMABE[1)], Takamasa KAYAMA[2)], Teiji TOMINAGA[1)]

1) Department of Neurosurgery, Tohoku University Graduate School of Medicine
2) Department of Neurosurgery, Yamagata University School of Medicine

The management of seven patients with choroid plexus tumors, 4 adults and 3 children (mean age 17.5 years) at our institution was reviewed. There were 4 cases of papilloma and 3 of carcinoma located in the lateral ventricle in 1 case, the third ventricle in 1 case, and the fourth ventricle in 5 cases. Total surgical excision was attempted in all patients. Total resection was achieved in three patients, resulting in no deficit in two and persistence of preoperative dysphagia in one. There was no recurrence after total resection. Subtotal resection was achieved in four patients, one of whom underwent second surgery resulting in total resection, and one patient died of respiratory disturbance after the third operation because of regrowth of the tumor. Complete excision could not be achieved in 3 of the 5 tumors located in the fourth ventricle because of extension to the brainstem. The median survival was 59.5 months for patients with papilloma, and 67.7 months for those with carcinoma. Adjuvant therapy was also required for carcinoma, one patient was treated by radiotherapy, and two by radiotherapy plus chemotherapy. Only one patient with papilloma was treated by radiotherapy plus chemotherapy postoperatively.

(Received : July 21, 2005, Accepted : September 14, 2005)

Key words choroid plexus tumor, total resection, radiotherapy, chemotherapy

No Shinkei Geka 34(1): 73-81, 2006

I. はじめに

脈絡叢乳頭腫/乳頭癌（choroid plexus tumor: CPT）は全頭蓋内腫瘍の0.4～1.0%程度といわれる稀な腫瘍である[3,15,22,24]．その好発年齢は2歳以下が全体の70%を占めると報告されており[3,5]，小児に多い[8,11,25]．好発部位は小児と成人で異なり，小児では側脳室，成人では第4脳室で多い[25]．脳室内に発生することがほとんどだが，稀に脳室外発生も報告されている[12,19]．治療に関しては，手術による全摘出の可否が予後にかかわるといわれるが[5,8,18,25]，補助療法については議論が分かれている．これまで単一施設での治療成績についてはいくつか報告があるが[2,3,6,8,13,15,16,18,22]，日本国内においては症例報告を散見するにとどまる[12,14]．本稿では当施設においてMRI導入以降

*(2005. 7. 21受稿，2005. 9. 14受理)

1）東北大学大学院神経外科学分野，2）山形大学医学部脳神経外科
〔連絡先〕隈部俊宏＝東北大学大学院神経外科学分野（〒980-8574 仙台市青葉区星陵町1-1）
Address reprint requests to : Toshihiro KUMABE, M.D., Department of Neurosurgery, Tohoku University Graduate School of Medicine, 1-1 Seiryo-machi, Aoba-ku, Sendai, Miyagi 980-8574, JAPAN
E-mail：kuma@nsg.med.tohoku.ac.jp

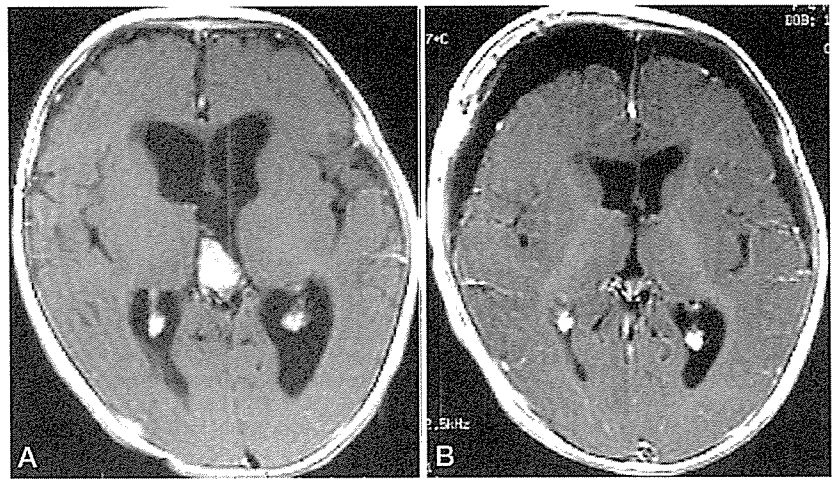

Fig. 1 Case 1, a 4-month-old girl with choroid plexus papilloma. Magnetic resonance (MR) imaging with gadolinium showed an enhanced mass in the third ventricle (**A**). The tumor was totally removed, but subdural fluid collection was seen after the surgery (**B**). She was treated with subdural-peritoneal shunting, and remained in good condition with no deficit.

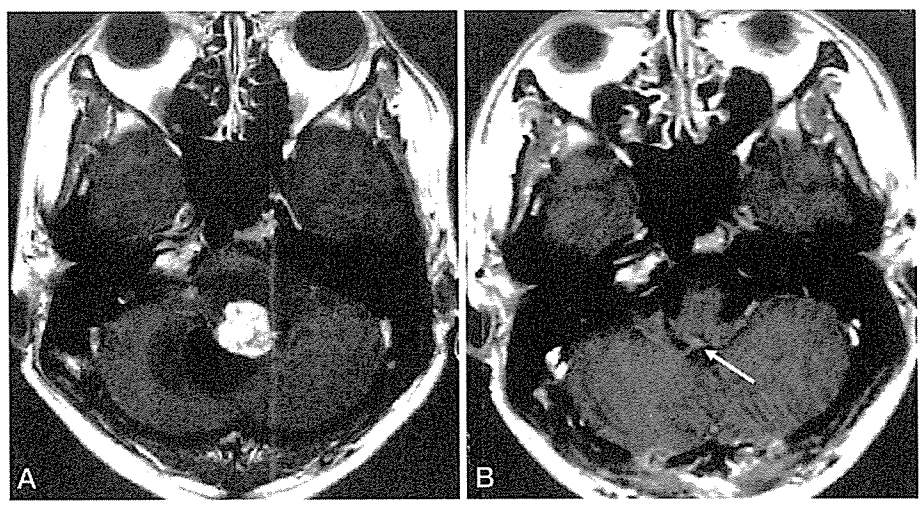

Fig. 2 Case 2, a 28-year-old male with choroid plexus papilloma. Magnetic resonance (MR) imaging with gadolinium showed an enhanced mass in the fourth ventricle (**A**). The tumor was removed subtotally and the residual tumor was observed as an enhanced spot (**B, arrow**). He had no deficit after the surgery and follow-up MR imaging detected no change in the size of the residual tumor.

の 1989 年より治療した CPT 7 症例の臨床経過について検討し，過去の文献的考察を加えて報告する．

II. 方法および結果

1989 年 MRI 導入以降，当施設において治療した脈絡叢乳頭腫(choroid plexus papilloma：CPP) 4 症例と脈絡叢乳頭癌（choroid plexus carcinoma：CPC）3 症例の計 7 症例（Case 1 ～ 7；**Fig. 1-7**）の経過および治療について検討を行った（**Table**）．年齢および性別については，CPP は 4 カ月女児(Case 1)，28 歳男性(Case 2)，29 歳女性(Case

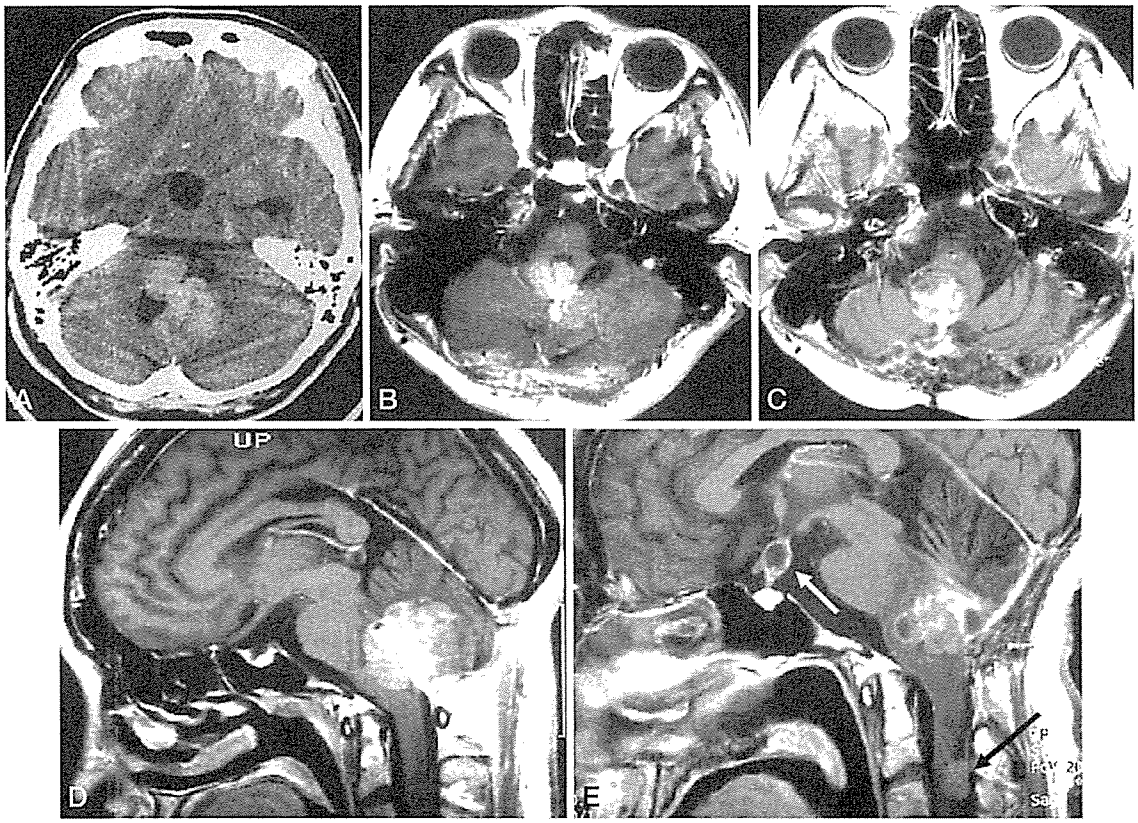

Fig. 3 Case 3, a 29-year-old female with choroid plexus papilloma. Computed tomography with contrast medium demonstrated the tumor in the fourth ventricle at presentation (**A**). Magnetic resonance (MR) imaging with gadolinium (**B**: axial, **D**: sagittal) at the first surgery showed the tumor was resected partially. However, MR imaging (**C**: axial, **E**: sagittal) at the second and third surgery with radiation and chemotherapy showed the tumor had enlarged and invaded the brainstem with dissemination in the cervical cord and third ventricle floor (**arrows, E**). She died of respiratory disturbance 56 months after the first surgery.

3), 37歳男性（Case 4), CPCは2カ月男児（Case 5), 3歳男児（Case 6), 25歳女性（Case 7）であった．腫瘍部位は側脳室が1症例，第3脳室が1症例，第4脳室が5症例であった．基本的治療方針としては可及的摘出を目標とした．側脳室と第3脳室に存在する症例では最終的には全摘出が可能であったが，第4脳室に存在する症例では脳幹への浸潤により全摘出は5例中2例にとどまった（Case 4, 6)．一方，CPP 4例のうち全摘出は2例，CPC 3例のうち全摘出は2例（うち1例は再手術により全摘出）と，手術摘出度と組織型の間に相関はなかった．

補助療法として，CPCの3例に対しては放射線療法あるいは化学療法を行った．3歳男児例（Case 6）については全脳全脊髄24 Gyと局所26 Gyの照射を行い，25歳女性例（Case 7）については全脳全脊髄30 Gyと局所24 Gyの照射およびACNUによる化学療法を併用した．2カ月男児例（Case 5）については若年であり，初回手術（亜全摘）後に補助療法は行わなかった．その後，残存腫瘍が増大したため再手術を施行している（全摘)．再手術時には術中照射（10 Gy）を併用し，術後は *in vitro* でのprimary cultureを用いた薬剤感受性試験にて有用性の確認されたvincristineおよびmethotrexateによる化学療法を行った[14]．CPPについては，脳幹部への広範な浸潤によ